

mmV2V: Combating One-hop Multicasting in Millimeter-wave Vehicular Networks

Jiangang Shen^{*}, Hongzi Zhu^{*§}, Yunxiang Cai^{*}, Bangzhao Zhai^{*}, Xudong Wang^{*}
 Shan Chang[†], Haibin Cai[‡], and Minyi Guo^{*}

^{*}Shanghai Jiao Tong University, China

[†]Donghua University, China

[‡]East China Normal University, China

{sjg19970410, hongzi, caiyunxiang, bangzhao, myguo}@sjtu.edu.cn wxudong@ieee.org
 changshan@dhu.edu.cn hbcai@esi.ecnu.edu.cn

Abstract—One-hop multicasting (OHM) of high-volume sensor data is essential for cooperative autonomous driving applications. While millimeter-Wave (mmWave) bands can be utilized for high-bandwidth OHM data transmission, it is very challenging for individual vehicles to find and communicate with a proper neighbor in a fully distributed and highly dynamic scenario. In this paper, we propose a fully distributed OHM scheme in vehicular networks, called mmV2V, which consists of three highly integrated protocols. Specifically, synchronized vehicles first conduct a probabilistic neighbor discovery procedure, in which randomly divided transmitters (or receivers) clockwise scan (or listen to) the surroundings in pace with heterogeneous Tx (or Rx) beams. In this way, the vast majority of neighbors can be identified in a few repeated rounds. Furthermore, vehicles negotiate with each of their neighbors about the optimal communication schedule in evenly distributed slots. Finally, each agreed pair of neighboring vehicles start high data rate transmissions with refined beams. We conduct extensive simulations and the results demonstrate that mmV2V can achieve a high completion ratio in rigid OHM tasks under various traffic conditions.

Index Terms—mmWave communication, one-hop multicasting, vehicular networks, beamforming, neighbor discovery

I. INTRODUCTION

As new vehicles are seeking higher levels of driving automation, more sophisticated sensors such as LIDAR and high-resolution cameras are equipped on such vehicles. The data rate of sensory data generated by a self-driving vehicle can be up to 750Mb/s [1] and traditional communication protocol working in low frequency band like 802.11p cannot undertake such heavy load. There is an urgent need for new V2V communication technology with higher bandwidth so that huge amount of sensory data can be exchanged among neighboring vehicles in real time [2]–[4]. As millimeter-wave (mmWave) bands in 60 GHz have about 14 GHz unlicensed spectrum, it exhibits a great potential for future V2V communications. We focus on the *one-hop multicasting* (OHM) problem in mmWave vehicular networks, *i.e.*, vehicles need to constantly exchange high-volume sensory data with a subset or all of their one-hop neighbors with narrow mmWave wireless beams. Figure 1 illustrates an OHM scenario, where vehicles equipped

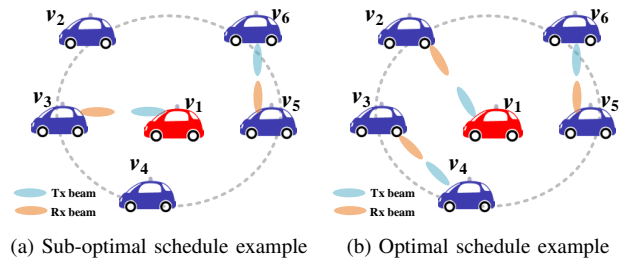


Fig. 1: An illustration of mmWave vehicular network, where data transmission only happens when a Tx beam is aligned with a Rx beam. In the OHM problem, each vehicle (*e.g.*, v_1) needs to individually communicate with its one-hop neighbors (*e.g.*, vehicles within the dotted disk area). Without centralized coordination, the network throughput may be sub-optimal as shown in (a) due to an inappropriate schedule.

with LIDAR exchange their individual 3D point cloud data with each of their one-hop neighbors via directional mmWave beams.

A practical OHM protocol in mmWave vehicular networks should satisfy three rigid requirements as follows. First, the protocol should fit in fully distributed settings due to the possible lack of a central unit such as a road side unit (RSU). Second, considering the characteristics of directional mmWave links, the protocol should maximize the number of aligned transmitter-and-receiver pairs and the corresponding link quality to achieve supreme network throughput. Last but not least, the protocol should be resilient to high mobility of vehicles which requires fast and frequent beam realignment.

In the literature, several pilot studies have demonstrated the feasibility of mmWave V2X communications. Wang *et al.* [1] deploy an experimental testbed consisting of one vehicle and four RSUs to enable microscopic investigation of the channel and the V2R link. Kim *et al.* [5] evaluate the performance of 802.11ad for V2V communication using a pair of vehicles. Such recent studies mainly focus on link-level measurements and have not considered the overall performance of the whole network. In traditional mmWave networks,

[§]Corresponding author

plenty of beam alignment schemes between multiple clients and Access Points (APs) have been proposed to increase the network throughput and robustness. BounceNet [6] is the first many-to-many mmWave beam alignment protocol that can exploit dense spatial reuse to allow many AP-to-client links to operate in parallel in a confined space and scale the wireless throughput with the number of clients. mmChoir [7] is a proactive blockage mitigation technique that utilizes joint transmissions from multiple APs to provide blockage resilience to clients. These protocols are designed for indoor scenarios and require centralized APs, which cannot be applied to fully distributed vehicular environments. As a result, there is no existing distributed protocol, to the best of our knowledge, that can successfully address the OHM problem in mmWave vehicular networks.

In this paper, we propose a fully distributed scheme, called *mmV2V*, which can effectively tackle the OHM problem in mmWave vehicular networks. The core idea of *mmV2V* is for individual vehicles to first efficiently discover their neighbors with directional Tx or Rx beams. More specifically, vehicles are synchronized and randomly choose to clockwise scan or listen to the surroundings in unison. Then, to determine an optimal neighbor to communicate, vehicles negotiate with their neighbors in evenly distributed time slots scheduled with a common hash function. Finally, an agreed pair of neighboring vehicles start to communicate with refined beams. The process repeats until a vehicle has exchanged data with all its neighbors.

There are two main challenges to be solved when designing *mmV2V*. First, the neighborhood of a vehicle is rapidly changing and hard to identify only with mmWave beams. Uncoordinated attempts from individual vehicles would only arouse signal collisions and unaligned beams. In *mmV2V*, vehicles are first synchronized via the Global Positioning System (GPS) and then conduct a probabilistic neighbor discovery procedure, consisting of multiple independent rounds. In each round, all vehicles can recognized one half of their neighbors without interfering with each other by letting all Tx and Rx beams scan in pace but with a 180° offset. As a result, after a small number of K rounds, a large ratio of $1 - 0.5^K$ neighbors can be identified. In addition, heterogeneous beam widths are used for Tx and Rx beams, respectively, to obtain an optimal discovery efficiency.

Second, in a fully distributed setting, it is very challenging for individual vehicles to collectively make a communication schedule that maximizes the whole network throughput. Indeed, to determine the optimal communication schedule is NP-hard even if the global network information is available. In order to tackle this challenge, *mmV2V* leverages a novel distributed greedy algorithm. In this algorithm, each vehicle negotiates about the optimal communication schedule with each of its neighbor according to a negotiation sequence of slots. The sequence is determined with a common hash function so that the same pair of neighbors are arranged to the identical slot but different pairs of neighbors are arranged to distinct slots. As a result, vehicles are coordinated to exchange

and update their individual decisions until they meet consensus after a few negotiation slots.

We conduct large-scale simulations where each vehicle performs a data exchange task requiring 200 Mbps data rate with its neighbors in various scenarios with different traffic densities. In normal traffic condition, *mmV2V* can complete 74.2% of the task, in contrast to 31.9% and 46.5% achieved by a random scheme and IEEE 802.11ad, respectively. The results demonstrate the efficacy of *mmV2V* design. We highlight the main contributions in this paper as follows: 1) a probabilistic neighbor discovery scheme without signal collisions is proposed; 2) a distributed greedy communication scheduling algorithm is proposed; 3) extensive simulations are conducted to demonstrate the efficacy of *mmV2V*.

II. SYSTEM MODEL AND PROBLEM DEFINITION

A. System Model

We consider more practical and challenging situation where there is no centralized control unit available. Vehicles move at variable speeds in the same direction on multi-lane surface roads and have equal capabilities as stated below:

- **Communication:** Each vehicle is equipped with a 60 GHz mmWave radio and a phased antenna array which can beam the signal with a desired beam width and in a desired direction according to multi-level codebooks. A co-channel deployment, uniform transmission power and half-duplex mode are assumed. V2V communications are operated under time division duplexing (TDD).
- **Synchronization:** Vehicles are synchronized through GPS receivers which can achieve high synchronization accuracy of less than 100 ns [8]. In addition, vehicles can also obtain their heading direction information with GPS receivers.
- **Computation:** Vehicles can perform basic calculations such as modulo operation and random number generation.

B. Problem Definition

Without the loss of generality, we consider those vehicles that have line-of-sight (LOS) path within the communication range of a vehicle v_i as its one-hop neighbors, denoted as \mathcal{N}_i . The OHM problem is to determine a communication schedule π such that the total time consumption for each vehicle $v_i \in V$ to exchange a unit of sensory data with selected or all its one-hop neighbors $v_j \in \mathcal{N}_i$ is minimized. We have the following theorem:

Theorem 1: *The OHM problem is NP-hard.*

Proof: Let $\mathcal{G} = \langle V, E \rangle$ denote the vehicular network, where $V = \{v_i, 1 \leq i \leq N\}$ is the set of vehicles and $E = \{l_{ij}, i \neq j\}$ is the set of LOS links between a pair of neighboring vehicles v_i and v_j . We assume that each vehicle v_i knows \mathcal{G} . With this graph, the OHM problem is equal to find a scheme π which can assign the minimum number of colors to all edges in E without assigning one color to any two or more edges connecting the same vehicle. This is the classic edge coloring problem which has been proved to be NP-complete [9]. In a fully distributed setting, the OHM is

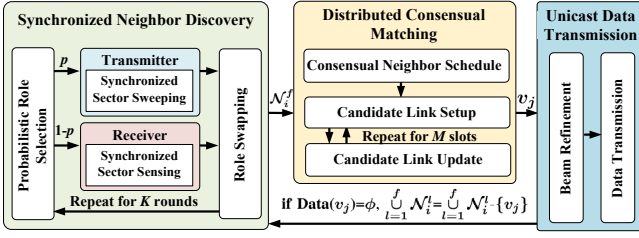


Fig. 2: Architecture of mmV2V.

even harder because it is difficult for each individual vehicle to obtain the global network information (e.g., the location information of each vehicle in the network) and coordinate with each other. This concludes the proof. ■

III. DESIGN OF MMV2V

A. Overview

In mmV2V, synchronized vehicles exchange their data in independent frames. In a frame f , all vehicles follow the same protocol, which consists of three components, i.e., synchronized neighbor discovery, distributed consensual matching, and unicast data transmission. Figure 2 depicts the architecture of mmV2V.

Synchronized Neighbor Discovery (SND). SND consists of multiple discovery rounds. In each round, a vehicle v_i first probabilistically selects a role as a transmitter or as a receiver. Then, all transmitters start to clockwise sweep the surroundings (divided into equal sectors) with wide transmission beams, and meanwhile all receivers start to sense on the corresponding opposite sector with wide reception beams. With this synchronized beam sweeping and sensing procedure, each receiver can efficiently collect the link information from those LOS transmitters without collisions. After that, vehicles swap their roles and conduct the synchronized beam sweeping and sensing procedure again. As a result, both ends of a LOS link make acquaintance to each other. With high probability, vehicle v_i can identify the vast majority of neighbors in the f th frame, denoted as \mathcal{N}_i^f , after a few number of discovery rounds.

Distributed Consensual Matching (DCM). Given all identified neighbors, DCM consists of a sequence of negotiation slots, during which each vehicle try to find the optimal neighbor for data transmission. In a distributed network setting, individual vehicles first perform the consensual neighbor schedule (CNS) that uses a Hash function to distribute neighboring vehicle pairs into different time slots to avoid packet collisions. In each slot, a vehicle v_i exchanges the information of its current candidate with the neighbor v_j designated by the CNS. If v_j is a better candidate in terms of maximizing the network throughput, v_i and v_j respectively set each other as their new candidates and update this change with their previous candidates.

Unicast Data Transmission (UDT). After consensual matching, vehicle v_i has determined which neighbor v_j to exchange data with. To obtain optimal data transmission rate,

v_i and v_j conduct fast beam refinement to search for the best narrow beam alignment, only within the range of the corresponding wide beam previously used for neighbor discovery. Then, they exchange a unit of data using the refined beams in the remaining time of this frame. If all sensory data have been exchanged with v_j , v_i removes v_j from $\bigcup_{l=1}^f \mathcal{N}_i^l$. After that, v_i repeats the whole process of mmV2V protocol until all sensory data have been exchanged with all its neighbors.

B. Synchronized Neighbor Discovery

In a fully distributed mmWave vehicular network, a vehicle needs to acquire precise location information of its neighboring vehicles, in order to conduct beam alignment for better link condition. However, it is challenging to efficiently identify neighbors only with non-broadcasting mmWave radios. One straightforward scheme is for a vehicle to decide to actively sweep its vicinity with beams or to passively listen as a receiver. As long as this maneuver repeats, each vehicle eventually can be acquainted with its neighborhood. Such a scheme cannot avoid interference of simultaneous beams aiming at the same receiver.

In mmV2V, neighbor discovery is coordinated among vehicle without being interfered with each other. Specifically, neighbor discovery consists of K rounds. In each round, a vehicle v_i performs a sequence of operations elaborated as follows:

1) *Probabilistic Role Selection:* Vehicle v_i first selects a role as a transmitter with the probability of p or as a receiver with the probability of $1 - p$. Given the independent role selection among vehicles, the whole network is expected to be separated with evenly distributed $N \cdot p$ transmitters and $N \cdot (1 - p)$ receivers, where N is the number of vehicles in the network.

2) *Synchronized Sector Sweeping:* After role selection, all transmitters are synchronized to clockwise sweep on a set of S predefined sectors with beams of α degrees wide measured at 3 dB attenuation. Sectors are indexed from the north direction, ranging from 0 to $S - 1$, and the interval of two consecutive sectors $\theta = 360^\circ / S$. When sweeping on a sector, a transmitter sends out its ID (e.g., MAC address) and the sector ID. As illustrated in Figure 3 (a), v_2 and v_3 select to be transmitters and their surroundings are equally divided into $S = 8$ sectors, with Sector 0 pointing at the north. Guided by the direction obtained from GPS receivers, v_2 and v_3 start to sweep from Sector 0 to Sector 7.

3) *Synchronized Sector Sensing:* Similarly, after role selection, all receivers are synchronized to clockwise sense on the same set of S predefined sectors but from the south sector (i.e., the opposite sector of the north sector), with beams of β wide. In general, if the current sweeping sector ID is i , the sensing sector ID is $(i + \frac{S}{2}) \% S$. When sensing a sector, a receiver passively listen from the reception beam. As illustrated in Figure 3 (a), v_1 selects to be a receiver and starts to sense on Sector 4 (i.e., the opposite sector of Sector 0). In this case, v_1 is roughly aligned with v_2 and can obtain v_2 's ID,

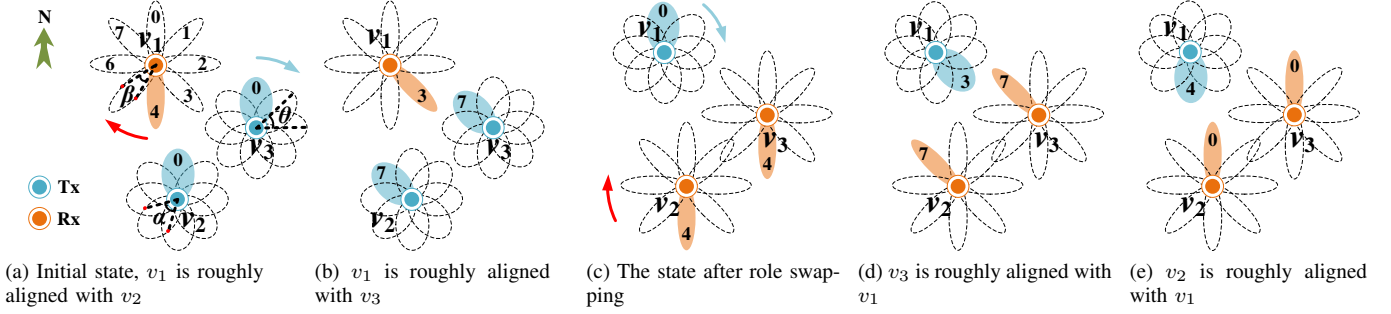


Fig. 3: Snapshots in an example of one synchronized neighbor discovery round, where v_1 selects to be a receiver and v_2 and v_3 select to be transmitters.

sweeping sector ID and the channel SNR information. With this synchronized sector sweeping and sensing scheme, all receivers can obtain the link information with all their LOS transmitters. For instance, as depicted in Figure 3 (b), v_1 gets to know about v_3 when the sweeping sector ID is seven and the sensing sector ID is three.

4) *Role Swapping*: After all sectors are swept or sensed, all vehicles swap their roles, *i.e.*, a transmitter becomes a receiver and vice versa, and respectively do the synchronized sector sweeping and sensing again. For example in Figure 3 (c), v_1 starts to sweep from Sector 0 and v_2 and v_3 start to sense from Sector 4. In this way, the LOS link information can be obtained by both ends of the link. For instance in Figure 3 (c) and (d), v_3 and v_2 also know about the LOS link with v_1 , respectively.

It should be noted that the settings of width of sweeping beams α and that of sensing beams β are a tradeoff between neighbor discovery efficiency and accuracy. With wider beams, the sweeping and sensing process consumes less time but coarser link measurement can be obtained. Moreover, with high probability, each vehicle can identify the vast majority of neighbors after a few number of discovery rounds. We have the following theorem:

Theorem 2: *If vehicles in the network use the same probability p to select a role, then $p = 0.5$ can make a vehicle identify the maximum number of LOS neighbors; after K*

discovery rounds, the expected ratio of identified neighbors is $1 - 0.5^K$ for $p = 0.5$.

Proof: For a vehicle v_i , a neighboring vehicle that cannot be identified by v_i after K discovery rounds is the vehicle that choose exactly the same roles as v_i for K times. Therefore, the probability for that to happen is $f(p, K) = [p^2 + (1-p)^2]^K$. To minimize $f(p, K)$, we have $\frac{df(p, K)}{dp} = 0$ which leads to $p = 0.5$. After K discovery rounds, the expected ratio of identified neighbors is $1 - [p^2 + (1-p)^2]^K$, which is $1 - 0.5^K$ for $p = 0.5$ and concludes the proof. ■

C. Distributed Consensual Matching

Given all identified neighbors, as stated in Theorem 1, the OHM problem is NP-hard. Without global network topology information, it is even harder for each vehicle to choose an optimal neighbor to communicate so that the whole network throughput is maximized. In mmV2V, each vehicle tries to achieve this goal in two steps as follows.

1) *Consensual Neighbor Schedule*: To avoid two or more neighboring vehicles simultaneously negotiating with the same vehicle, each vehicle arranges a negotiation sequence of M slots. For vehicle v_i , it schedules vehicle $v_j \in \mathcal{N}_i^f$ to the k th slot if $(H(MAC(v_i)) + H(MAC(v_j)))\%C = k\%C$, for $k \in [0, M-1]$, where $H(\cdot)$ is a Hash function; $MAC(\cdot)$ returns the MAC address of a vehicle; and C is a constant used to separate vehicles in \mathcal{N}_i^f into different slots. For example, as illustrated in Figure 4(a), we assume that v_2 has a LOS path with v_1 and v_3 , respectively, and $M = 3, C = 3, (H(MAC(v_1)) + H(MAC(v_2)))\%3 = 2$ and $(H(MAC(v_2)) + H(MAC(v_3)))\%3 = 0$. In this case, v_1 and v_2 will both schedule each other to Slot 2, and v_2 and v_3 will both schedule each other to Slot 0.

Note that when M is larger than C , vehicle $v_j \in \mathcal{N}_i^f$ can be arranged in v_i 's sequence for multiple times. The purpose of this is for both vehicles to update their decisions (see below). If there are more than one vehicles in \mathcal{N}_i^f being assigned to the same slot due to Hash collision or a small C , v_i will random pick one to fill the slot.

2) *Candidate Link Setup and Update*: Vehicle v_i negotiates with its neighbors one by one according to the determined negotiation sequence. Specifically, in each slot, if there is a vehicle $v_j \in \mathcal{N}_i^f$ is scheduled in that slot, v_i and v_j

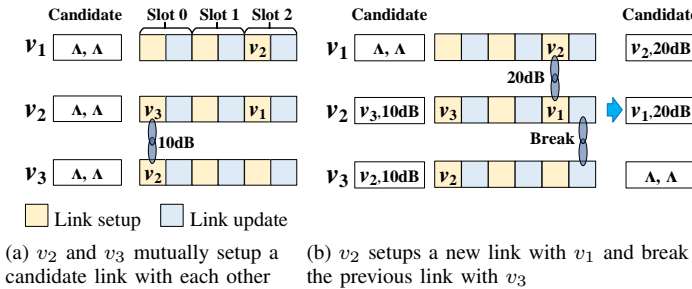


Fig. 4: An illustration of distributed consensual matching, where v_2 has a LOS path with v_1 and v_3 , respectively and $M = 3, C = 3$.

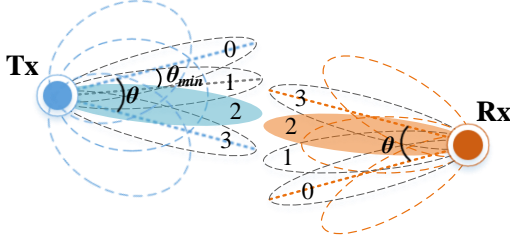


Fig. 5: An illustration of beam refinement, where the optimal narrow beams can be aligned via cross searching.

will exchange the link quality information of their current communication candidates¹. Both vehicles will set each other as the new communication candidate if one of the following conditions stands: 1) both v_i and v_j have no candidates; 2) v_i (or v_j) has a candidate v_l but the quality of the link between v_i and v_j is better than the candidate link between v_i (or v_j) and v_l . Otherwise, v_i and v_j keep their current candidates unchanged. In addition, for the second condition, v_i (or v_j) will also update with v_l to inform v_l that v_i (or v_j) is no longer its candidate.

For example in Figure 4(a), in Slot 0, both v_2 and v_3 have no current candidate. After exchange this information, both vehicles record each other as the current candidate and the SNR of the link (e.g., 10 dB) as shown in the left part of Figure 4(b). In Slot 2, as the quality of the link between v_2 and v_1 (e.g., 20 dB) is better than that of the link between v_2 and v_3 , v_2 changes its candidate from v_3 to v_1 and informs v_3 with this change during the second half of Slot 2, as shown in the right part of Figure 4(b).

D. Unicast Data Transmission

After distributed consensual matching, a vehicle v_i has determined which neighbor v_j is optimal to exchange data with. However, v_i and v_j are coarsely aligned with wide beams. To further obtain better data transmission rate, v_i and v_j conduct beam refinement to search for the best alignment with the narrowest beams. Specifically, as illustrated in Figure 5, the number of narrowest beams needed to search on each side is $s = \lfloor \frac{\theta}{\theta_{min}} \rfloor + 1$, where θ is the sector interval as stated in Section III-B2 and θ_{min} is the interval of narrow beams. As s is usually very small, v_i and v_j find the best narrow beam alignment via cross searching. Finally, they exchange a unit of data with the refined narrowest beams.

IV. PERFORMANCE EVALUATION

A. Methodology

We use VENUS [10], which is a vehicular network simulator supporting microscope transportation simulations, to generate road traffic of different density on a road segment of 1km long with three lanes of 5m wide on each direction.

¹Both vehicles follow a rule to transmit their information in turn. For example, the vehicle with a larger MAC address does first.

The speed range on three lanes is 40–60km/h, 50–70km/h, and 60–80km/h, respectively. The simulator calculates the location of each vehicle based on a car-following model and a lane-changing model. We adopt the standard long-distance path loss model [11], which is formulated as

$$g_{i,j}^l = a \cdot 10 \cdot \log_{10} d + O + 15 \cdot d/1000, \quad (1)$$

where d is the distance between v_i and v_j ; a represents the path loss exponent; O is a constant determined by the number of blockers; and the last term is atmospheric attenuation. We utilize a beam pattern based on a 3GPP channel model [12], which defines the antenna gain at orientation γ as

$$g^a(\gamma) = \begin{cases} g^1 10^{-\frac{3}{10}(\frac{|\gamma|}{\omega/2})^2} & |\gamma| < \theta_1 \\ g^2 & \theta_1 < |\gamma| < \pi \end{cases}, \quad (2)$$

where ω is the 3 dB beam width; g^1 and g^2 are the main lobe gain and side lobe gain, respectively; and $\theta_1 = \omega/2\sqrt{10/3\log_{10}(g^1/g^2)}$ is the boundary of the main lobe and the side lobe. We set Tx and Rx beam width (α and β) to 30° and 12° respectively. Assume v_j receives data from v_i , the SINR measured at v_j at time t is calculated as

$$SINR_{i,j}(t) = \frac{p_i(t)g_i^a(t)g_{i,j}^c(t)g_j^r(t)}{N_0B + \sum_{k \in N_j, k \neq i} p_k(t)g_k^a(t)g_{k,j}^c(t)g_j^r(t)} \quad (3)$$

where $p_i(t) = 28$ dBm is v_i 's transmission power; $g_i^a(t)$ and $g_j^r(t)$ are antenna gain of v_i and v_j , respectively; $N_0 = -174$ dBm/Hz is the Gaussian noise power density; and $B = 2.16$ GHz is the bandwidth of the channel. We adopt the Modulation and Coding Scheme (MCS) of IEEE 802.11ad protocol [13], which support a data transmission rate up to 4.62Gbps. IEEE 802.11ad provides MCS0 for control PHY, MCS1-12 for data transmission with Single Carrier (SC). For each MCS, 802.11ad provides the required Error Vector Magnitude (EVM) calculated as $SINR^{-1/2}$ [14]. A frame lasts for 20ms. The 802.11ad Sector level Sweep (SSW) frame is used when doing synchronized sector sweeping, which takes 15 μ s [15]. The delay for forming a new beam is set to 1 μ s. For scanning 24 sectors, one round of SND takes 0.8ms. The candidate link setup and link update in a negotiation slot takes 4.3 μ s, respectively, which is equal to `aControlPHYPreAmbleLength`. The time needed for receiving and processing a frame is 3 μ s which is equal to `aSIFSTime` defined in 802.11ad [13]. One negotiation slot in DCM takes 0.03ms. Vehicle position and link quality is updated every 5ms in all simulations.

We consider a typical application of 3GPP video data sharing for assisted and improved automated driving (VaD) [16], referred to as *high resolution image exchange* (HRIE) task, which requires 100-700 Mbps data rate for exchanging video data (with resolution 1280 x 720, 24 bit per pixel, 30 fps).

We compare the overall performance of mmV2V with the following two schemes:

- **Random OHM Protocol (ROP):** ROP adopts the random neighbor discovery and matching schemes, respectively. In neighbor discovery scheme, each vehicle randomly selects a role (*e.g.*, Tx or Rx) and a direction to cast a Tx or Rx beam. When a Tx beam is aligned with a Rx beam, the corresponding Tx vehicle is identified by the Rx vehicle. In matching scheme, each vehicle randomly selects a neighbor. A pair of vehicles are matched if they are both unmatched before and choose each other.
- **IEEE 802.11ad:** The IEEE 802.11ad protocol can be directly utilized for solving the OHM problem. In our experiments, frames are set to be 20ms and the probability that one vehicle chooses to be PCP is set to 30%. After receiving several beacons sent by PCPs, a vehicle will randomly choose a PBSS to join in.

We consider the following three metrics to evaluate the performance of all candidate schemes:

- **OHM Completion Ratio (OCR):** Let \mathcal{N}_i^C denote the set of neighboring vehicles that have completed data exchange with v_i . OCR of v_i is calculated as $\frac{|\mathcal{N}_i^C|}{|\mathcal{N}_i|}$.
- **Average of Transmission Progress (ATP):** Let $D_{i,j}$ denote the amount of data that have exchanged between v_i and v_j , and let $\eta_{i,j}$ denote the transmission progress between v_i and v_j , *i.e.*, $\eta_{i,j} = \frac{D_{i,j}}{D}$. ATP of v_i , denoted as $\bar{\eta}_i$, reflects the average progress of data exchange between v_i and its neighbors, calculated as $\bar{\eta}_i = \frac{1}{|\mathcal{N}_i|} \sum_{v_j \in \mathcal{N}_i} \eta_{i,j}$.
- **Deviation of Transmission Progress (DTP):** DTP of v_i is calculated as $\sqrt{\frac{\sum_{v_j \in \mathcal{N}_i} |\eta_{i,j} - \bar{\eta}_i|^2}{|\mathcal{N}_i|}}$, which measures the fairness of communication opportunities among its neighbors. A small DTP value means that v_i tends to exchange data with its neighbors equally.

B. Parameter Configuration

1) *Effect of the Constant C:* In this experiment, we explore the capability of the constant C (and together the hash function) to separate neighbors in different negotiation slots. Similarly, we generate traffic of different densities. In each traffic setting, we vary the value of C from one to twelve with an interval of one, and calculate the average communication capacity per vehicle over the whole network after a certain number of negotiation slots.

Figure 6 plots the capacity per vehicle as a function of the number of negotiation slots under four different traffic scenarios. The average number of neighbor \mathcal{N}_i of the generated traffic is five, six, seven, and eight, respectively. It can be seen that when C is small, *e.g.*, it requires more negotiation slots before a high capacity is achieved. The reason is that given a small C , a vehicle v_i would likely cast more than one neighbors into the same negotiation slot and randomly pick one to negotiate, which means that the negotiation decisions could be inconsistent among vehicles and hurts the matching efficiency per slot. This can be remedied by increasing the number of negotiation slots. On the contrary, a large C would waste many negotiation slot unassigned. As a result, it would

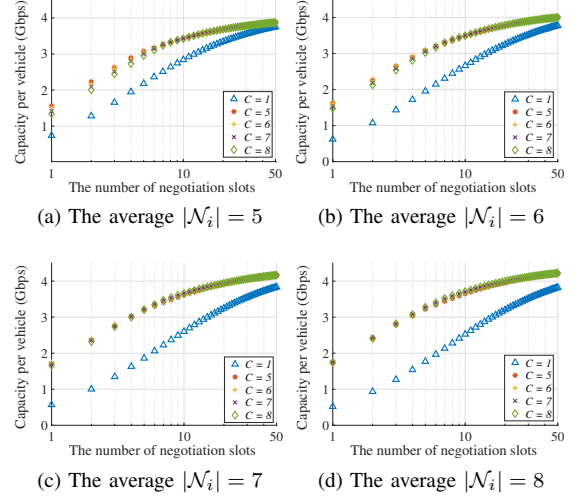


Fig. 6: The capability of the constant C to separate neighbors in different negotiation slots.

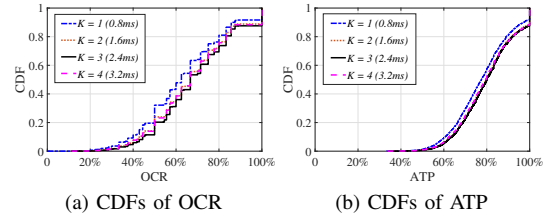


Fig. 7: Effect of the number of discovery rounds K .

be ideal if $C = |\mathcal{N}_i|$ as seen from Figure 6. Since $|\mathcal{N}_i|$ varies, $C = 7$ is a good practice.

2) *Effect of the Number of Neighbor Discovery Rounds K:* In this experiment, we study the effect of the number of neighbor discovery rounds K . We generate traffic of different densities as above experiments and set the number of negotiation slots M equal to 40. In each traffic setting, we vary k from one to four with an interval of one and repeat the experiment for one hundred times.

Figure 7 plots the cumulative density function (CDF) of OCR and ATP, respectively, obtained with different neighbor discovery rounds when the traffic density is 20 vpl. It can be seen from the figure that when $K = 3$ mmV2V achieves the best performance. The reason is that the SND protocol is a probabilistic neighbor discovery method. Using more discovery rounds will find more neighbors but also spends more time. A good tradeoff is $K = 3$, according to Theorem 2, the expected ratio of identified neighbors in a single frame is 87.5%. Note that after 3 frames 99.8% of neighbors can be discovered. Similar results are seen in other traffic scenarios.

3) *Effect of the Number of Negotiation Slots M:* We explore the effect of the number of negotiation slots M in this experiment. The settings of this experiment are similar to the experiment above except we set $K = 3$ and vary the number of negotiation slots from 20 to 80 with an interval of

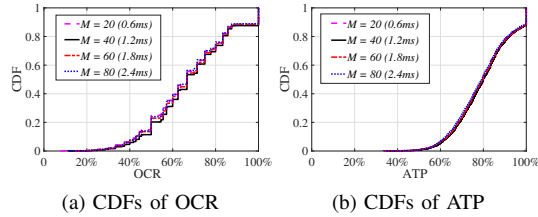


Fig. 8: Effect of the number of negotiation slots M

20. OCR and ATP are calculated at the end of every second.

Figure 8 plots the CDF of OCR and ATP with different M . It is clear to see that when $M = 40$ the performance of mmV2V is the best. The reason is that insufficient negotiation slots will lead to suboptimal matching results whereas an overwhelming number of negotiation slots only waste much time without bringing more matched pairs. As a result, we choose $M = 40$ as an optimal configuration.

It should be noted that since neighbor discovery and distributed matching phase takes very short time (less than 5ms in total), therefore vehicular topology can be treated as stationary during these phases in one frame.

C. Performance Comparison

We compare mmV2V as a whole OHM protocol with ROP and IEEE 802.11ad in different traffic scenarios. In each traffic setting, we set $\alpha = 30^\circ$, $\beta = 12^\circ$, $\theta = 15^\circ$, $C = 7$, $K = 3$, and $M = 40$. Vehicle performs a 200 Mbps *HRIE* task. Figure 9 plots three metrics as functions of the traffic density. It can be seen that mmV2V can achieve a high average OCR of 74.2% when the traffic density is 15 vpl (*i.e.*, the distance D between a pair of vehicle on a lane is about 66 meters). In contrast, the average OCR achieved by ROP and 802.11ad at the same traffic density are 31.9% and 46.5%, respectively. Even when the traffic density reaches 30 vpl ($D = 33$ meters), the average OCR achieved by mmV2V is 57.6%, comparing to 22.7% and 19.2% obtained by ROP and 802.11ad, respectively. Furthermore, from Figure 9(c), it can be seen that when traffic density and the corresponding workload is low, mmV2V can complete the *HRIE* task among most vehicles, leading to small DTP values. When the traffic density is high, mmV2V prefers to complete data exchange between vehicles with better link quality, resulting a higher DTP.

V. RELATED WORK

Traditional mmWave Networks: Beam alignment is a classic topic in researches about mmWave networks [17]–[21]. Hassanieh *et al.* [17] utilized multi-armed beams and proposed a hash-based algorithm to decrease the complexity of beam searching. Their result demonstrated that the best beam can be founded in a logarithmic number of measurements. Hashemi *et al.* [22] modeled the beam alignment problem as an online stochastic optimization problem and utilized a contextual MAB model to solve it. Their algorithm is proved to be asymptotically optimal. Haider *et al.* [20] calculated the

best beam direction on device by tracking indicator LEDs on Wireless APs and no beam training is required. These beam alignment algorithms mainly focus on beam alignment between two nodes.

Plenty of research is done to increase the throughput and robustness of the communication in mmWave networks. Jog *et al.* [6] proposed a protocol called BounceNet which conduct many-to-many beam alignment between multiple APs and clients and calculate a communication combination with minimum interference. Zhang *et al.* [7] proposes a protocol called mmChoir to tackle the problem of blockage occurring in mmWave networks by letting multiple APs transmit to the clients simultaneously. Wei *et al.* [23] proposed a 60 GHz network architecture called Pia which employs pose information on mobile devices, together with a multi-AP network architecture, to achieve seamless coverage in mmWave networks. Experiment results show that BounceNet, mmChoir and Pia can increase the performance of mmWave network. However, all of these protocols are all designed for indoor scenarios and requires centralized APs.

mmWave communication in VANET: Some works utilize side-channel information to help beam alignment in VANET. Va *et al.* [24] utilized GPS information to aid beam prediction. Gonzalez-Prelcic *et al.* [25] utilized the channel information of mmWave radar to help conduct beam alignment. However these works only focus on beam alignment in VANET.

Wang *et al.* [1] deployed an experimental testbed consisting of one vehicle and four RSUs to enable microscopic investigation of the channel and the V2R link. From extensive measurement, they found that beam management can be handled easily if the codebook is properly designed. Moreover, highly effective spatial multiplexing can be realized with aligned transmission and reception beams. However, their work only investigates the characteristics of mmWave links in vehicular environments. Kim *et al.* [5] placed commercial 802.11ad products on two vehicles and conducted real-world experiments to evaluate the performance of 802.11ad in V2V communications, their results demonstrated that link quality is mainly effected by vehicle speed and distance between vehicles. However, their work only investigates the data transmission between two vehicles.

The most relevant work to our scheme is the matching scheme proposed by Perfecto *et al.* [26]. This work proposed a distributed association and beam alignment scheme in mmWave VANETs, where vehicles are matched based on a utility function. However, this work mainly considers the matching strategy without considering how to efficiently schedule vehicles in a distributed network setting.

VI. CONCLUSION

In this work, a fully distributed OHM scheme in vehicular networks, called mmV2V, has been proposed. In mmV2V, vehicles can efficiently discover their one-hop neighbors with directional beams. Moreover, individual vehicles can collectively make a communication schedule to achieve appealing network throughput. We have conducted extensive simulations

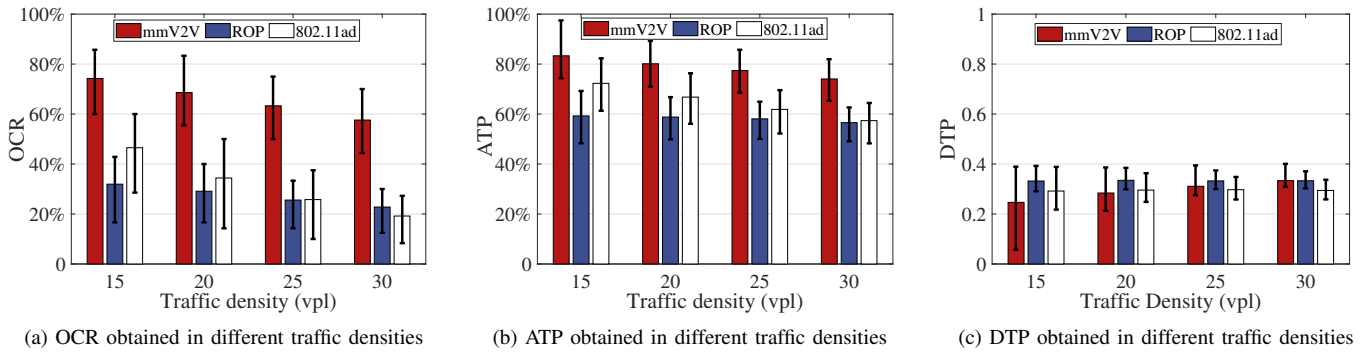


Fig. 9: Comparison of different OHM protocols.

and the results demonstrate that mmV2V can achieve a high completion ratio in rigid OHM tasks under various traffic conditions.

ACKNOWLEDGEMENTS

This research was supported in part by National Key RD Program of China (Grants No. 2018YFC1900700), National Natural Science Foundation of China (Grants No. 61872240 and 61972081), the Natural Science Foundation of Shanghai (Grant No. 22ZR1400200), STIC (CJGJZD20210408092400001) and the Fundamental Research Funds for the Central Universities.

REFERENCES

- [1] S. Wang, J. Huang, and X. Zhang, "Demystifying Millimeter-Wave V2X: Towards Robust and Efficient Directional Connectivity under High Mobility," in *Proceedings of ACM MobiCom*, 2020.
- [2] F. Ahmad, H. Qiu, R. Eells, F. Bai, and R. Govindan, "CarMap: Fast 3D Feature Map Updates for Automobiles," in *Proceedings of USENIX NSDI*, pp. 1063–1081, 2020.
- [3] W. Yi, Y. Liu, Y. Deng, A. Nallanathan, and R. W. Heath, "Modeling and Analysis of MmWave V2X Networks With Vehicular Platoon Systems," *IEEE Journal on Selected Areas in Communications*, vol. 37, no. 12, pp. 2851–2866, 2019.
- [4] H. Qiu, F. Ahmad, F. Bai, M. Gruteser, and R. Govindan, "AVR: Augmented Vehicular Reality," in *Proceedings of ACM MobiSys*, p. 81–95, 2018.
- [5] W. Kim, "Experimental Demonstration of MmWave Vehicle-to-Vehicle Communications Using IEEE 802.11ad," *Sensors*, vol. 19, no. 9, 2019.
- [6] S. Jog, J. Wang, J. Guan, T. Moon, H. Hassanieh, and R. R. Choudhury, "Many-to-Many Beam Alignment in Millimeter Wave Networks," in *Proceedings of USENIX NSDI*, pp. 783–800, 2019.
- [7] D. Zhang, M. Garude, and P. H. Pathak, "mmChoir: Exploiting Joint Transmissions for Reliable 60GHz MmWave WLANs," in *Proceedings of ACM MobiHoc*, p. 251–260, 2018.
- [8] H. A. Omar, W. Zhuang, and L. Li, "VeMAC: A TDMA-Based MAC Protocol for Reliable Broadcast in VANETs," *IEEE Transactions on Mobile Computing*, vol. 12, no. 9, pp. 1724–1736, 2013.
- [9] I. Holyer, "The np-completeness of edge-coloring," *SIAM J. COMPUT.*, vol. 10, no. 4, pp. 718–720, 1981.
- [10] "Vehicular Networking Universal Simulator." <http://lion.sjtu.edu.cn/project/projectDetail?id=17>.
- [11] A. Yamamoto, K. Ogawa, T. Horimatsu, A. Kato, and M. Fujise, "Path-Loss Prediction Models for Intervehicle Communication at 60 GHz," *IEEE Transactions on Vehicular Technology*, vol. 57, no. 1, pp. 65–78, 2008.
- [12] J. Wildman, P. H. J. Nardelli, M. Latva-aho, and S. Weber, "On the Joint Impact of Beamwidth and Orientation Error on Throughput in Directional Wireless Poisson Networks," *IEEE Transactions on Wireless Communications*, vol. 13, no. 12, pp. 7072–7085, 2014.
- [13] "IEEE Standard for Information technology–Telecommunications and information exchange between systems–Local and metropolitan area networks–Specific requirements–Part 11: Wireless LAN Medium Access Control (MAC) and Physical Layer (PHY) Specifications Amendment 3: Enhancements for Very High Throughput in the 60 GHz Band," *IEEE Std 802.11ad-2012 (Amendment to IEEE Std 802.11-2012, as amended by IEEE Std 802.11ae-2012 and IEEE Std 802.11aa-2012)*, pp. 1–628, 2012.
- [14] H. A. Mahmoud and H. Arslan, "Error vector magnitude to SNR conversion for nondata-aided receivers," *IEEE Transactions on Wireless Communications*, vol. 8, no. 5, pp. 2694–2704, 2009.
- [15] P. Zhou, X. Fang, Y. Fang, Y. Long, R. He, and X. Han, "Enhanced Random Access and Beam Training for Millimeter Wave Wireless Local Networks With High User Density," *IEEE Transactions on Wireless Communications*, vol. 16, no. 12, pp. 7760–7773, 2017.
- [16] 3GPP, "Study on enhancement of 3GPP Support for 5G V2X Services (Release 16)," Technical Report (TR) 22.886, 3rd Generation Partnership Project, 2018. V16.2.0.
- [17] H. Hassanieh, O. Abari, M. Rodriguez, M. Abdelghany, D. Katabi, and P. Indyk, "Fast Millimeter Wave Beam Alignment," in *Proceedings of ACM SIGCOMM*, pp. 432–445, 2018.
- [18] M. E. Rasekh, Z. Marzi, Y. Zhu, U. Madhoo, and H. Zheng, "Non-coherent MmWave Path Tracking," in *Proceedings of ACM HotMobile*, p. 13–18, 2017.
- [19] N. J. Myers, A. Mezghani, and R. W. Heath, "Swift-Link: A Compressive Beam Alignment Algorithm for Practical mmWave Radios," *IEEE Transactions on Signal Processing*, vol. 67, no. 4, pp. 1104–1119, 2019.
- [20] M. K. Haider, Y. Ghasempour, D. Koutsonikolas, and E. W. Knightly, "LiSteer: MmWave Beam Acquisition and Steering by Tracking Indicator LEDs on Wireless APs," in *Proceedings of ACM MobiCom*, p. 273–288, 2018.
- [21] J. Palacios, D. Steinmetzer, A. Loch, M. Hollick, and J. Widmer, "Adaptive Codebook Optimization for Beam Training on Off-the-Shelf IEEE 802.11ad Devices," in *Proceedings of ACM MobiCom*, p. 241–255, 2018.
- [22] M. Hashemi, A. Sabharwal, C. Emre Koksall, and N. B. Shroff, "Efficient Beam Alignment in Millimeter Wave Systems Using Contextual Bandits," in *Proceedings of IEEE INFOCOM*, pp. 2393–2401, 2018.
- [23] T. Wei and X. Zhang, "Pose Information Assisted 60 GHz Networks: Towards Seamless Coverage and Mobility Support," in *Proceedings of ACM MobiCom*, p. 42–55, 2017.
- [24] V. Va, X. Zhang, and R. W. Heath, "Beam Switching for Millimeter Wave Communication to Support High Speed Trains," in *Proceedings of IEEE 82nd Vehicular Technology Conference (VTC-Fall)*, pp. 1–5, 2015.
- [25] N. González-Prelcic, R. Méndez-Rial, and R. W. Heath, "Radar aided beam alignment in MmWave V2I communications supporting antenna diversity," in *Proceedings of Information Theory and Applications Workshop (ITA)*, pp. 1–7, 2016.
- [26] C. Perfecto, J. Del Ser, and M. Bennis, "Millimeter-Wave V2V Communications: Distributed Association and Beam Alignment," *IEEE Journal on Selected Areas in Communications*, vol. 35, no. 9, pp. 2148–2162, 2017.